Am J Physiol Lung Cell Mol Physiol 286: L1311–L1318, 2004.
First published February 20, 2004; 10.1152/ajplung.00394.2003.

Altered bleomycin-induced lung fibrosis in osteopontin-deficient mice

Jeffrey S. Berman,[1,2] David Serlin,[1] Xinfang Li,[1] Geoffrey Whitley,[1] John Hayes,[3] David C. Rishikof,[1] Dennis A. Ricupero,[1] Lucy Liaw,[4] Margaret Goetschkes,[5] and Anthony W. O'Regan[1]

[1]*The Pulmonary Center, Boston University School of Medicine, Boston 02118;* [2]*The Pulmonary Department, Boston Veterans Administration Medical Center, Boston 02132;* [3]*Department of Pathology, Boston University School of Medicine, Boston 02118;* [5]*Pathology Services, Incorporated, Cambridge, Massachusetts 02139; and* [4]*Center for Molecular Medicine, Maine Medical Center Research Institute, Scarborough, Maine 04074*

Submitted 18 November 2003; accepted in final form 12 February 2004

Berman, Jeffrey S., David Serlin, Xinfang Li, Geoffrey Whitley, John Hayes, David C. Rishikof, Dennis A. Ricupero, Lucy Liaw, Margaret Goetschkes, and Anthony W. O'Regan. Altered bleomycin-induced lung fibrosis in osteopontin-deficient mice. *Am J Physiol Lung Cell Mol Physiol* 286: L1311–L1318, 2004. First published February 20, 2004; 10.1152/ajplung.00394.2003.—Osteopontin is a multifunctional matricellular protein abundantly expressed during inflammation and repair. Osteopontin deficiency is associated with abnormal wound repair characterized by aberrant collagen fibrillogenesis in the heart and skin. Recent gene microarray studies found that osteopontin is abundantly expressed in both human and mouse lung fibrosis. Macrophages and T cells are known to be major sources of osteopontin. During lung fibrosis, however, osteopontin expression continues to increase when inflammation has receded, suggesting alternative sources of ostepontin during this response. In this study, we demonstrate immunoreactivity for osteopontin in lung epithelial and inflammatory cells in human usual interstitial pneumonitis and murine bleomycin-induced lung fibrosis. After treatment with bleomycin, osteopontin-null mice develop lung fibrosis characterized by dilated distal air spaces and reduced type I collagen expression compared with wild-type controls. There is also a significant decrease in levels of active transforming growth factor-β_1 and matrix metalloproteinase-2 in osteopontin null mice. Type III collagen expression and total collagenase activity are similar in both groups. These results demonstrate that osteopontin expression is associated with important fibrogenic signals in the lung and that the epithelium may be an important source of osteopontin during lung fibrosis.

pulmonary fibrosis; type I collagen; matrix metalloproteinase-2; transforming growth factor-β

OSTEOPONTIN IS A MATRICELLULAR protein abundantly expressed during inflammation and repair (11). Originally considered a bone matrix protein, recent studies showed that osteopontin also functions as a cytokine regulating macrophage accumulation and type I cytokine expression at sites of injury and infection (11, 32). Osteopontin is expressed in usual interstitial pneumonitis (UIP), fibrotic lung granulomas, and multiple models of murine lung fibrosis including transgenic overexpression of tumor necrosis factor-α and intratracheal challenge with bleomycin (19, 28, 32, 37, 41). Recent cDNA microarray studies identified osteopontin as one of several genes markedly upregulated during human UIP and bleomycin injury in mice (19, 41). Compared with normal lung, osteopontin expression was increased 12-fold in lung tissue from patients with UIP and 27-fold in mouse lungs following bleomycin challenge. The sites and cellular sources of osteopontin during lung fibrosis are unknown.

Osteopontin expression begins during the inflammatory stage of bleomycin injury in mice but progressively increases to peak levels during lung fibrosis (19, 37). Mice carrying a null mutation in the epithelial-restricted integrin-β_6 develop inflammation in response to intratracheal bleomycin but are protected from lung fibrosis, largely due to failure of transforming growth factor (TGF)-β1 activation at epithelial surfaces (19). Osteopontin expression is markedly attenuated following bleomycin injury in β_6-integrin null mice (19). Thus osteopontin expression correlates with fibrosis rather than inflammation during postinflammatory lung fibrosis in mice. Osteopontin null (−/−) mice have been shown to develop abnormal postinflammatory repair and fibrosis in the heart, kidney, and skin (24, 38). Osteopontin deficiency is associated with a predominance of small-caliber collagen fibrils and reduced type I collagen deposition (24, 38). Osteopontin can also modulate the expression of matrix metalloproteinases (MMP)-1, -2, and -9 as well as fibroblast proliferation and migration in vitro (11, 18, 34, 35, 37, 39). Based on the known functions of osteopontin, we hypothesized that it may modulate cellular accumulation and collagen depostion and remodeling during lung fibrosis.

Lung fibrosis involves excessive lung fibroblast proliferation, extracellular matrix remodeling, and architectural distortion due to a complex interaction between numerous factors such as TGF-β and MMPs (36). Intratracheal administration of bleomycin sulfate in susceptible strains of mice induces lung fibrosis. Recent studies demonstrated close similarities in cellular gene and protein expression between the two responses (19, 41). Nevertheless, differences in the mechanism and physiological consequences of fibrosis between this model and UIP impede direct comparisons of these responses (7).

Our present studies demonstrate the expression of osteopontin protein in human and murine lung fibrosis and describe the effects of osteopontin deficiency on pulmonary fibrosis induced by bleomycin challenge in vivo. Osteopontin immunoreactivity was present in inflammatory and epithelial cells during lung fibrosis. Compared with osteopontin-sufficient mice, osteopontin −/− mice developed lung fibrosis characterized by cystic dilatation of distal airways and a reduction in type I collagen expression. In the absence of osteopontin expression, there was decreased nonlatent or active TGF-β1 as well as total and active MMP-2 expression. These results show

Address for reprint requests and other correspondence: A. O'Regan, Pulmonary Center, R-304, Boston Univ. School of Medicine, 715 Albany St., Boston, MA 02118 (E-mail: aoregan@lung.bumc.bu.edu).

The costs of publication of this article were defrayed in part by the payment of page charges. The article must therefore be hereby marked "*advertisement*" in accordance with 18 U.S.C. Section 1734 solely to indicate this fact.

that osteopontin expression is associated with important fibrogenic signals in the lung. The association of osteopontin with lung epithelium and important mediators of the cellular response to lung epithelial injury suggests that the epithelium may be an important source and target for osteopontin during lung fibrosis.

MATERIALS AND METHODS

Tissue samples and bleomycin treatment. Archived lung tissue from five patients with idiopathic pulmonary fibrosis was used as approved by the Institutional Review Board of the Boston Veterans Administration Medical Center. The hisotological presence of UIP was confirmed by a pathologist using standard criteria (1). Mouse studies were approved by the Institutional Animal Care and Use Committee at Boston University School of Medicine. The generation and baseline characterization of osteopontin −/− mice (deletion of exon 4–7 on 129SVJ × Black Swiss background) were previously described, and the genotype of all mice was confirmed by PCR analysis (24). Specific pathogen-free male and female homozygous osteopontin −/− mice or age- and sex-matched wild-type littermate controls (8–12 wk, weight 20–28 g) were challenged intratracheally (IT) with either bleomycin sulfate (Blenoxane, Bristol-Myers Squibb) or sterile saline. As there are strain variations in the response to IT bleomycin, we performed preliminary experiments with a range of doses of bleomycin from 0.03 to 0.1 units. These experiments showed that the 129SVJ background was moderately sensitive to bleomycin with doses over 0.03 units resulting in a high mortality rate due to acute lung injury by *day 8*. Doses of 0.03 units resulted in lung fibrosis with an early mortality of <10%. Thus all experiments were performed on groups of five to seven mice using 0.03 units of IT bleomycin. Histology was assessed at 8 and 16 days, and all other analysis was performed at 16 days.

Histology. After fixation in 4% paraformaldehyde and routine processing, the extent of fibrosis was assessed by percent involvement, and the severity of fibrosis was assessed using a modified Ashcroft score: 1 = minimal fibrosis; 2 = moderate fibrosis with thickening of the alveolar walls but no architectural distortion; 3 = fibrosis with definite damage to the lung structure and formation of fibrous bands; and 4 = severe distortion of structure with large fibrous areas (including honeycomb lung) (4). Cellularity was graded histologically and by bronchoalveolar lavage (BAL) cell counts. The number and size of epithelial lined cysts were measured using a tissue micrometer at ×100 magnification in eight random fibrotic sites per mouse lung. Results were reported as mean size (μm) and mean number of cystic spaces per high-power field. Histological analysis was performed by a pathologist (J. Hayes) blinded to the experimental conditions.

Immunohistochemistry. For immunohistochemistry (IHC), following antigen retrieval with citrate buffer, tissue sections were stained as previously described with the following primary antibodies: human lung biopsies with mouse anti-rat osteopontin MAb, MPIIIB10 (1:150 dilution, Iowa Hybridoma Bank); mouse lungs with *1*) goat anti-rat osteopontin, Op199 pAb (20 μg/ml), *2*) rat anti-mouse monocyte/macrophage marker F4/80 (1:5 dilution, Serotec), *3*) goat anti-mouse type I collagen polyclonal antibodies raised against fetal mouse skin (1:25 dilution, Calbiochem), and *4*) goat anti-human type III collagen (10 μg/ml; Chemicon International, Temecula, CA) (14, 31, 32, 38). Control slides were incubated with appropriate normal serum or isotype-matched MAb. Staining was read as either positive or negative except for type I collagen where it was graded as follows: immunoreactivty: 0 = none; 1 = minimal; 2 = moderate; and 3 = intense staining. All histology was assessed in a blinded manner.

BAL. BAL was performed on mice 16 days after bleomycin or saline challenge. Ice-cold sterile PBS with 0.1 mM EDTA was infused IT in aliquot volumes of 700 μl and aspirated. This was repeated until a 4-ml vol was recovered from each mouse. BAL was then centrifuged at 300-*g* force (1,200 rpm) for 10 min, the resultant cell pellet was resuspended in 1 ml of PBS. Total cells were counted using a microcytometer. After cytospin (40,000 cells/sample) and staining with Hema 3 stain set (123–869, Fisher Diagnostics, Middletown, VA), differential cell counts were performed by counting 400 cells in each BAL sample.

Protein isolation. Lungs were first perfused with 10 ml of ice-cold PBS, excised, weighed, and frozen in liquid nitrogen. Lungs were then homogenized in Triton solution (0.25% Triton X-100 in 10 mM $CaCl_2$) at a concentration of 20 ml Triton solution/g lung tissue. Final lung homogenate volumes were normalized to total protein concentration as measured by Bradford assay and stored at −20°C.

RNA isolation and Northern blot analysis. Total lung cellular RNA was isolated by guanidine thiocyanate-phenol-chloroform extraction (10). RNA loading was assessed by ethidium bromide staining of ribosomal bands and by cohybridization with GADPH. The α_1(I) collagen cDNA probe was derived from a rat α_1(I) collagen cDNA that specifically binds murine α_1(I) collagen mRNA (13).

Total collagen, TGF-β1 ELISA, and collagenase assay. Total lung-soluble collagen was measured using the Sircol assay (Accurate Chemical and Scientific) as previously described (16). One-hundred microliters of total lung homogenate were assayed for collagen content and results were expressed per milligram of lung. Equal amounts of total protein from lung homogenates were assessed for latent and nonlatent TGF-β1 by ELISA (TGF-β1 E_{max} ImmunoAssay System, Promega). This ELISA has been used previously to measure lung total and bioactive (nonlatent) TGF-β1 in mice with a reported sensitivity of 32 pg/ml (21). Similarly, equal amounts of total protein from lung homogenates were assessed for collagenase activity using the Chemicon MMP collagenase activity kit (ECM710, Chemicon International), which measures cleavage of bovine biotinylated collagen using a streptavidin-enzyme complex. This collagen substrate is readily cleaved by MMP-1, -8, and -13, as well as enzymes with less specific collagenase activity such as elastases. Lung homogenate total collagenase activity was expressed relative to a standard curve constructed with serial concentrations of activated human MMP-1 (range 1–6 ng/ml) supplied by the manufacturer.

Gelatin zymography. Gelatinolytic activity was assessed in lung homogenates using gelatin zymography as previously described (23). Equal amounts of total protein (20 μg) from lung homogenates were mixed with sample buffer in the absence of reducing agent and then loaded and run on a 10% SDS-polyacrylamide gel containing gelatin (concentration 0.5 mg/ml) for 90 min. The gel was then incubated in renaturing buffer (cat. no. LC2670, Invitrogen, Carlsbad, CA) for 60 min and then in developing buffer (cat. no. LC2671, Invitrogen) for 48 h at 37°C. Nondigested gelatin was then stained with 0.1% Coomassie brilliant blue (Sigma). Negative staining showed areas of gelatinolytic activity typical of MMP-2 and -9 between 60 and 92 kDa. The relative amount and ratio of activated to total MMP-2 were measured by densitometry (ChemiImager System and AlphaEase software, Alpha Ionotech, San Leandro, CA).

Statistical analysis. Results are expressed as means ± SD. Means ± SE are used where results from several experiments are reported together. Student's *t*-test was used to compare two groups of animals, whereas ANOVA with post hoc analysis using Newman-Keuls test was used where appropriate in multiple group comparisons. $P < 0.05$ was considered significant.

RESULTS

Expression of osteopontin in human UIP and murine bleomycin-induced lung fibrosis. Using IHC, we showed abundant expression of osteopontin protein in lung biopsies demonstrating UIP. In all cases, immunoreactivity for osteopontin was seen exclusively in cellular components of the fibrotic response and not the fibrotic matrix (Fig. 1, *A–D*). Positive staining was

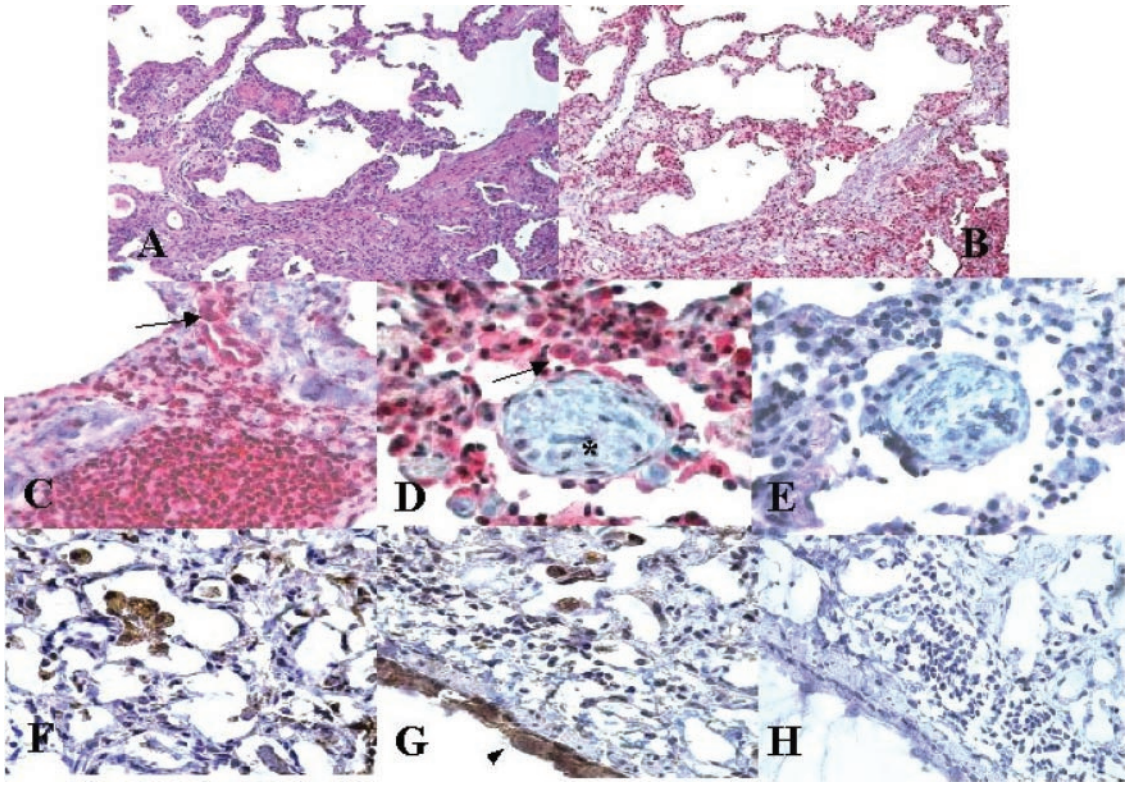

Fig. 1. Expression of osteopontin in lung fibrosis. *A–E*: lung biopsy showing usual interstitial pneumonitis. *A*: hematoxylin and eosin stain reveals typical interstitial fibrosis with scattered foci of inflammation and considerable lung architectural distortion (×100). *B*: serial section stained with antiosteopontin MAb reveals extensive immunoreactivitiy (staining red) for osteopontin in the cellular but not the fibrotic matrix of the response (×100). Section is counterstained with hematoxylin. *C*: a high-power view shows bronchiolar and alveolar epithelial cells (arrow) as well as an inflammatory infiltrate composed of lymphocytes and macrophages staining positively for osteopontin (×200). The associated fibrosis is negative. *D*: hyperplastic cuboidal type II alveolar cells (arrow) also demonstrate prominent immunoreactivity for osteopontin (×400). No osteopontin signal is present in fibroblast foci (*). *E*: there is no immunoreactivity in a serial section stained with isotype control MAb (×400). *F–H*: bleomycin-induced lung fibrosis in mice (×400). Osteopontin immunoreactivity (brown staining) is present in alveolar macrophages (*F*) and airway epithelium (arrowhead; *G*). *H*: no immunoreactivity is present in the serial section stained with isotype control antibody.

seen in macrophages, lymphocytes, and both bronchiolar and alveolar epithelium (Fig. 1, *C* and *D*). No staining was seen when an isotype control antibody was used (Fig. 1*E*). Cubiodal epithelial cells typical of hyperplastic type II pneumocytes exhibited strong immunoreactivity for osteopontin (Fig. 1, *C* and *D*). There was no osteopontin signal in fibroblast foci (Fig. 1*D*). As we previously reported, osteopontin immunoreactivity was present in some alveolar macrophages but not airway epithelium or type II pneumocytes in normal human lung (not shown) (31). We next characterized the expression of osteopontin in postinflammatory lung fibrosis 16 days after bleomycin challenge in mice, a time we previously showed to be associated with established lung fibrosis in this strain of mice (Fig. 2*C*). Again, osteopontin signal was present in macrophages and epithelial cells but not the fibrotic matrix (Fig. 1, *F* and *G*). No staining was seen when an isotype control antibody was used (Fig. 1*H*). Consistent with prior reports, osteopontin immunoreactivity was not present in normal mouse lung (not shown) (37). Thus epithelia and macrophages demonstrate immunoreactvity for osteopontin in UIP and bleomycin-induced lung injury in mice.

Osteopontin −/− mice develop cystic lung fibrosis in response to bleomycin challenge. At early stages (*day 8*), bleomycin induced diffuse pulmonary inflammation and alveolitis in both osteopontin +/+ and osteopontin −/− mice. This was characterized by prominent inflammatory infiltrates composed of lymphocytic aggregates and macrophages. By *day 16*, lung injury was characterized by diffuse fibrosis with persistent but decreased inflammatory cell infiltrates of macrophages and lymphocytes (Fig. 2, *C–F*). Lung fibrosis was diffuse but predominantly peribronchiolar and subpleural, although considerable heterogeneity was present with some mice exhibiting fibrosis of almost the entire lobe (fibrosis % lung involvement: osteopontin +/+: 23 ± 18%, mean ± SD, vs. osteopontin −/−: 31 ± 26%, mean ± SD; modified Ashcroft score: osteopontin +/+: 2.33 ± 0.5, mean ± SD, vs. osteopontin −/−: 2.5 ± 0.4, mean ± SD; $n = 15$, $P = 0.3$). These findings are typical of bleomycin-induced lung fibrosis in mice and were similar in osteopontin +/+ and osteopontin −/− mice. There was also no significant difference between the numbers of inflammatory cells between the groups of mice (Fig. 3*A*). In particular, the numbers of macrophages as measured by BAL cell count (Fig. 3*A*) and lung IHC for the macrophage marker F4/80 (not shown) were similar in osteopontin +/+ and osteopontin −/− mice.

There was an increase in the number of cystic epithelial lined air spaces within the fibrotic areas of lung in osteopontin −/− mice compared with osteopontin +/+ controls (Figs. 2,

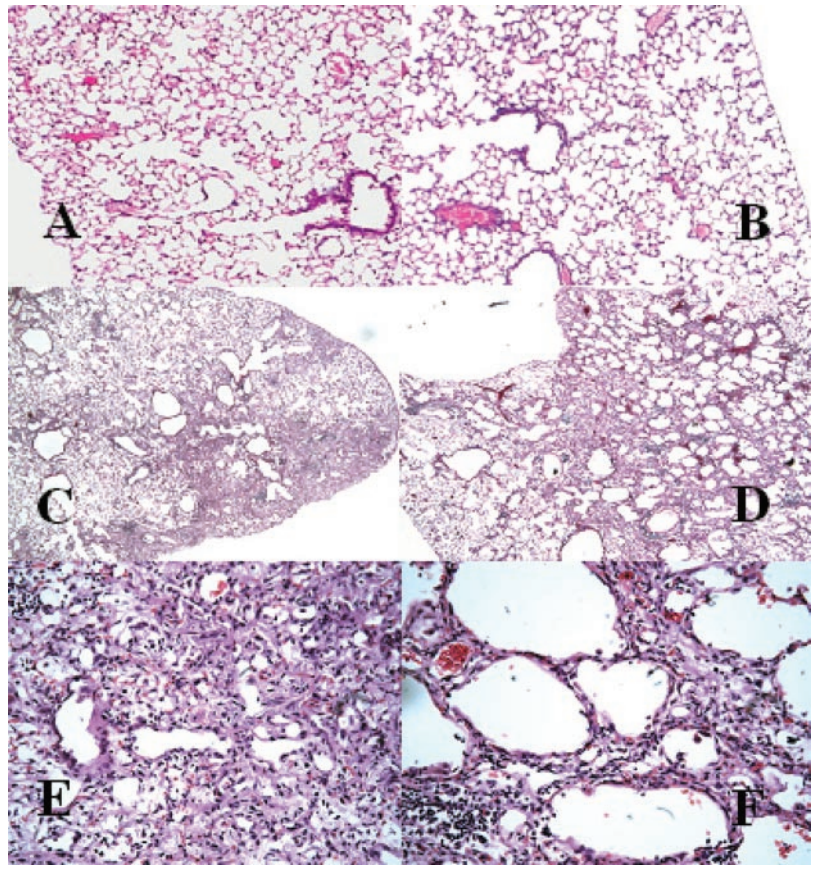

Fig. 2. Bleomycin-induced lung fibrosis in osteopontin −/− and osteopontin +/+ mice. Lungs from osteopontin +/+ (*A*, *C*, *E*) and osteopontin −/− (*B*, *D*, *F*) mice are shown 16 days after saline (*A*, *B*) or bleomycin (*C–F*) challenge. There is no difference in lung morphology, architecture, or inflammation after saline challenge in osteopontin +/+ (*A*) compared with osteopontin −/− (*B*) mice. *C*: after bleomycin challenge, osteopontin +/+ mice develop typical diffuse peribronchiolar and subpleural fibrosis with prominent interstitial infiltration with mixed inflammatory cells (×100). *E*: high-power view confirms these findings and reveals small dilated terminal air spaces within the matrix (×400). *D*: in osteopontin −/− mice, there is also extensive peribronchial and subpleural disease with fibrosis and inflammation (×100). In contrast to control mice, osteopontin deficiency is associated with the development of numerous cystic spaces within the fibrotic areas (×100). *F*: on high-power view, these spaces appear to be lined by epithelium (×400). The diameter of terminal bronchioles is not different between osteopontin +/+ and osteopontin −/− mice. These images are representative of 3 experiments (n = 15/group).

C–F, and 3*B*). There were 11.6 ± 2 (mean ± SD) spaces per ×100 field in osteopontin −/− mice compared with 5.5 ± 3 (mean ± SD) spaces per high-power field in osteopontin +/+ mice (P = 0.004; Fig. 3*B*). In addition to an increase in number, these air spaces were also more dilated in osteopontin −/− mice. The average diameter of the cystic spaces in osteopontin −/− was 1,090 ± 210 μm (mean ± SD) compared with 880 ± 96 μm (mean ± SD) in osteopontin +/+ mice (P = 0.04; Fig. 3*B*). There was no significant difference in the number or size of terminal bronchioles in osteopontin −/− compared with osteopontin +/+ mice. Results are representative of three experiments (n = 15/group).

Reduced type I collagen expression in response to bleomycin challenge in osteopontin −/− mice. Total collagen levels in lungs from mice 16 days after bleomycin challenge showed increased collagen deposition in both osteopontin +/+ and osteopontin −/− mice compared with saline-treated controls (percent increase over saline 153 ± 22%, mean ± SD, in osteopontin +/+ mice vs. 117 ± 21%, mean ± SD, in osteopontin −/− mice; Fig. 3*C*). Collagen accumulation was less in osteopontin −/− mice compared with osteopontin +/+ mice, but this was not statistically significant (osteopontin +/+ 6.2 ± 0.9 μg·mg lung^{-1}, mean ± SD, vs. osteopontin −/− 5.5 ± 1.3 μg·mg lung^{-1}, mean ± SD; n = 6, P = 0.1). There was, however, a significant decrease in type I collagen between the two sets of mice (Fig. 4, *A* and *B*). By IHC, there was decreased expression of type I collagen in the fibrotic response seen in osteopontin −/− mice compared with osteopontin +/+ controls (IHC grade: osteopontin +/+ 2.5 ± 0.1, mean ± SD, vs. osteopontin −/− 1.4 ± 0.15, mean ± SD; n = 8, P = 0.004; Fig. 4, *A* and *B*). In contrast, type III collagen expression was similar in both sets of mice (Fig. 4, *C* and *D*).

These findings could reflect deceased expression type I collagen or increased degradation by type I collagenases that are widely expressed during lung fibrosis (36). By Northern blot analysis of total lung mRNA, we showed that α_1 (I) collagen mRNA expression was similar at baseline in both sets of mice but was significantly higher in osteopontin +/+ (osteopontin +/+ 0.75 ± 0.1 relative densitometry to GAPDH, mean ± SD) compared with osteopontin −/− mice (0.35 ± 0.25, mean ± SD, relative densitometry to GAPDH; n = 3, $P < 0.05$) following bleomycin treatment (Fig. 5). In contrast, there was no difference in collagenase activity between osteopontin −/− and osteopontin +/+ bleomycin-treated mice (osteopontin −/− 116 ± 20 ng/ml, mean ± SD, vs. osteopontin +/+ 122 ± 18 ng/ml, mean ± SD, of MMP-1 activity per mg of lung, n = 6, P = 0.25).

Osteopontin −/− mice have reduced active TGF-β1 expression during bleomycin-induced lung fibrosis. TGF-β1 is a potent stimulator of type I collagen production and so we next determined whether the expression of TGF-β1 was altered in these mice. By ELISA we found a significant decrease in nonlatent or active TGF-β1 levels in whole lung homogenates obtained during the fibrotic phase of bleomycin-induced lung injury. In three experiments involving a total of 16 mice per group, nonlatent TGF-β1 levels were 1,043 ± 144 pg/ml (mean ± SE) in osteopontin +/+ mice compared with 606 ± 97 pg/ml (mean ± SE) in osteopontin −/− mice (P = 0.015; Fig. 5). There was a small but nonsignificant decrease in total TGF-β in osteopontin −/− compared with osteopontin +/+

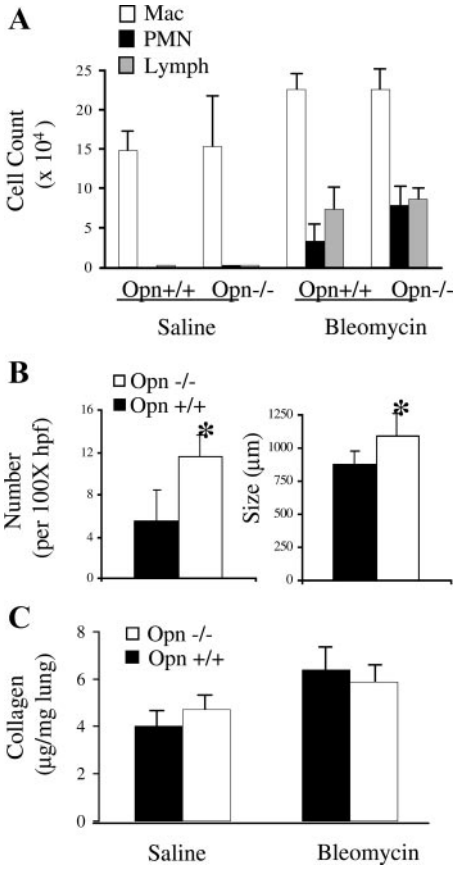

Fig. 3. *A*: macrophage (Mac), neutrophil (PMN), and lymphocyte (lymph) counts from bronchoalveolar lavage samples obtained 16 days after saline or bleomycin treatment. There is no significant difference between osteopontin +/+ and osteopontin −/− mice (n = 6/group). *B*: number and size of cystic spaces within areas of fibrosis in osteopontin +/+ and osteopontin −/− mice. Osteopontin deficiency is associated with a significant increase in the number and size of cystic areas within the fibrotic lung (*$P < 0.05$). Data are representative of 3 experiments (n = 15/group). *C*: total collagen levels in lungs harvested 16 days after saline or bleomycin treatment. In both osteopontin +/+ and osteopontin −/− mice, there is an increase in collagen level after bleomycin challenge. There is no significant difference between the groups of mice (n = 6/group). hpf, High-power field; Opn, osteopontin.

mice (osteopontin +/+ 2,171 ± 545 pg/ml, mean ± SE, vs. osteopontin −/− 1,753 ± 689 pg/ml, mean ± SE; $P = 0.35$). No significant differences were found in either total or active TGF-β levels in saline-treated control animals (active TGF-β: osteopontin +/+ 132 ± 120 pg/ml, mean ± SE, vs. osteopontin −/− 92 ± 85 pg/ml, mean ± SE; $P = 0.35$).

Reduced expression and activation of MMP-2 in osteopontin −/− mice. Similar to collagenases, gelatinases are expressed during murine bleomycin-induced lung fibrosis and may regulate several aspects of lung fibrosis including TGF-β activation (23, 40). In view of these data, we next assessed gelatinase activity in bleomycin-treated osteopontin −/− and osteopontin +/+ mice. Compared with saline-treated controls, bleomycin treatment resulted in increased expression and activation of both MMP-2 and -9 in both groups of mice. However, there was a significant decrease in MMP-2 expression in osteopontin −/− mice compared with osteopontin +/+ mice (gelatinolytic activity: osteopontin +/+ 6,291 ± 1,200, mean ± SD, vs. osteopontin −/− 2,167 ± 510, mean ± SD; $n = 5$, $P < 0.05$; Fig. 6). There was also a significant decrease in active MMP-2 in osteopontin −/− mice (gelatinolytic activity: osteopontin +/+ 2,304 ± 800, mean ± SD, vs. osteopontin −/− 689 ± 350, mean ± SD; $n = 5$, $P < 0.05$; Fig. 6). This represented a significant reduction in the percent active form of MMP-2 (osteopontin +/+ 36 ± 4%, mean ± SE, vs. osteopontin −/− 32 ± 2%, mean ± SE, $n = 10$, $P < 0.05$). Expression of MMP-9 was similar in osteopontin +/+ and osteopontin −/− mice (data not shown). Results are representative of two experiments (n = 10 per group).

DISCUSSION

In these studies, we show immunoreactivity for osteopontin in epithelial cells and inflammatory cells during lung fibrosis. In addition, mice deficient in osteopontin expression develop altered bleomycin-induced lung fibrosis characterized by cystic dilated air spaces, decreased type I collagen expression, and a reduction of active TGF-β1 and MMP-2.

We found osteopontin immunoreactivity in inflammatory and epithelial cells but not the fibrotic matrix in UIP. Similar

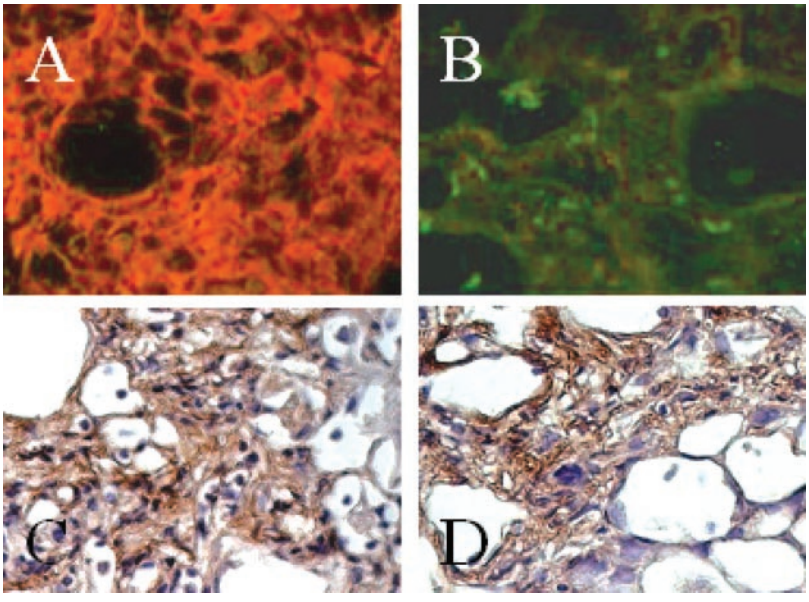

Fig. 4. Type I collagen expression in mice 16 days after bleomycin exposure. *A* (osteopontin +/+) and *B* (osteopontin −/−) show the expression of type 1 collagen (red) using immunohistochemistry at *day 16* (×200). Intense staining (grade 3) for type 1 collagen is present in osteopontin +/+ mice compared with minimal staining (grade 1) in osteopontin −/− mice. In contrast, type III collagen expression (brown) is similar in osteopontin +/+ (*C*) and osteopontin −/− (*D*) mice.

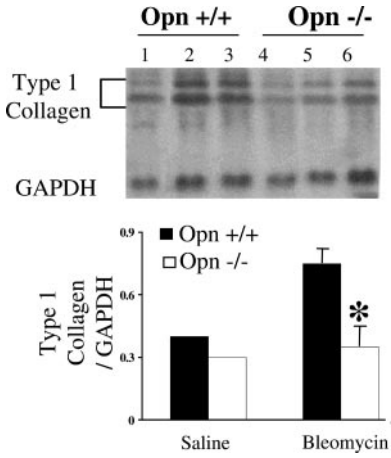

Fig. 5. *Top*: Northern blot analysis of α_1 (1) collagen mRNA expression in whole lung mRNA isolated 16 days after bleomycin exposure. Results from 6 mice are shown: *lane 1*, osteopontin +/+ saline; *lanes 2* and *3*, osteopontin +/+ bleomycin; *lane 4*, osteopontin −/− saline; *lanes 5* and *6*, osteopontin −/− bleomycin. *Bottom*: by densitometry and compared with GAPDH expression, there is significantly less upregulation of α_1 (1) collagen mRNA after bleomycin challenge in osteopontin −/− mice compared with osteopontin +/+ mice (means ± SD from 3 mice/group, $*P < 0.05$).

results were found in postinflammatory lung fibrosis induced by bleomycin in mice. Our results suggest that the lung epithelium may be an important source of osteopontin in response to epithelial injury and lung fibrosis. This is consistent with known expression of osteopontin by epithelial cells lining the bronchial, gastrointestinal, and genitourinary tracts (8). As well as bronchiolar epithelium we found osteopontin immunoreactivity in hyperplastic type II pneumocytes. In UIP, distal airway and alveolar epithelial cells undergo cuboidalization and hyperplasia and are prominent sources of fibrogenic cytokines such as TGF-β1 and platelet-derived growth factor BB (3, 20, 36). They may also provide critical signals to induce fibroblasts to migrate, proliferate, and ultimately develop a profibrotic phenotype (36). These results show that osteopontin is part of the epithelial response during lung fibrosis and suggest that it may play a role in epithelial repair and regeneration during lung fibrosis.

Some studies in osteopontin-deficient mice have shown altered inflammatory cell and, in particular, macrophage, accumulation as well as Th1 cytokine expression during inflammatory responses such as granulomatous inflammation (5, 9, 30, 32). Others involving wound repair and myocardial infarction have shown normal inflammation but aberrant fibrosis (24, 38). We show that despite normal macrophage accumulation, there is aberrant lung fibrosis in the absence of osteopontin. The nature of the lung injury may account for these different results. Models of granulomatous inflammation are usually intravenously delivered, causing a gradually evolving hypersensitivity response (22). In contrast, IT bleomycin results in acute severe epithelial damage followed by acute lung injury and fibrosis (36). It is possible that different signals and mediators regulate inflammatory cell recruitment in these types of lung inflammatory responses.

Several studies have shown prominent osteopontin expression during postinflammatory lung fibrosis in mice, and osteopontin can augment platelet-derived growth factor BB-induced lung fibroblast proliferation and migration in vitro (19, 28, 37). We now show that osteopontin deficiency is associated with altered fibrosis characterized by increased numbers of cystic air spaces. These findings may reflect airway dilatation due to an altered fibrotic response similar to the postinfarction-dilated cardiomyopathy that was recently reported in osteopontin −/− mice (38). Fibrosis characterized by cystic dilatation of distal air spaces has been described in mice following cadmium injury in a process that can be exacerbated by inhibiting the lysyl oxidase enzyme (29). Therefore, abnormal collagen matrix assembly can result in air space dilatation. Interestingly, electron microscopy has shown abnormal collagen fibril composition in both the heart and skin of osteopontin −/− mice (24, 38). We did not perform ultrastructural analysis, but our findings of reduced type I collagen expression in fibrotic osteopontin-deficient lungs are similar to that reported in cardiac postinflammatory fibrosis in osteopontin −/− mice (38). Collectively, these studies suggest that osteopontin may be required to develop a typical fibrotic scar with adequate tensile strength to prevent airway dilatation. A recent study demonstrated that deficient activation of TGF-β resulted in increased MMP-12 expression with associated airway dilatation and emphysema (27). Further studies are necessary to clarify the relationship of osteopontin deficiency to these findings.

Collagen deposition reflects a balance among expression, remodeling, and degradation of collagen matrix (36). Net collagen accumulation is regulated by TGF-β expression and activation as well as the presence and activity of various collagenases. We found that there was a decrease in α_1 (I) collagen mRNA and no increase in collagenase activity in osteopontin −/− mice. The expression of type III collagen, another major fibrillar collagen expressed during lung fibrosis, was not different between the two sets of mice. These data suggest that there may be a specific deficiency in type I collagen expression in osteopontin −/− mice.

TGF-β is the major stimulus for type I collagen expression during lung fibrosis. In bleomycin lung injury, the activity of

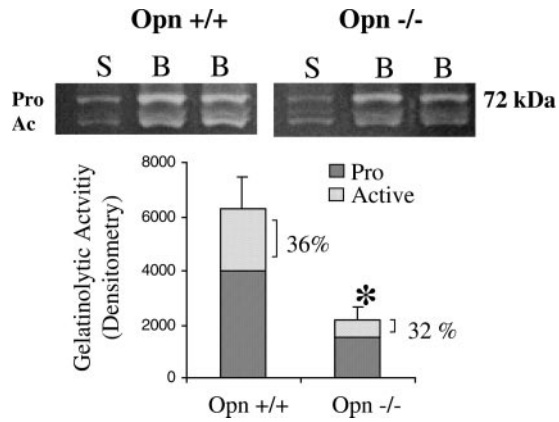

Fig. 6. Gelatinolytic activity of lung homogenates from osteopontin +/+ and osteopontin −/− mice. Lung homogenates were assessed using gelatin zymography. Typical gelatinolysis consistent with matrix metalloproteinase (MMP)-2 was detected at 72 kDa. Compared with saline (S) treatment, bleomycin (B) induces MMP-2 activity in both osteopontin +/+ and osteopontin −/− mice. There was a reduction in total and active (Ac) MMP-2 in osteopontin −/− mice compared with osteopontin +/+ mice. Using densitometry, these differences are significant ($*P < 0.05$). Data are from 2 experiments involving a total of 10 mice/group. Pro, pro-MMP-2.

TGF-β is regulated at both transcriptional and posttranslational levels during bleomycin-induced lung injury. We demonstrated a reduction in active TGF-β1 but not total TGF-β in osteopontin −/− mice. Although osteopontin has previously been shown to be a TGF-β1 response gene, our data suggest that osteopontin may in fact function upstream of TGF-β_1 by regulating its activation (11, 12, 17, 19, 26). A prior study showed that total TGF-β1 was reduced in osteopontin −/− mice following renal tubulointerstitial injury, but this has not been reported in other organs, and no prior study has shown a reduction in TGF-β1 activation (30). The activation of TGF-β from its latency-associated peptide (LAP) can involve conformational shifts due to the interaction of LAP with thrombospondin and integrins or proteolytic cleavage by MMPs and plasmin (2, 40). The β_6-integrin is a critical activator of TGF-β1 in experimental lung fibrosis, and osteopontin expression is dramatically attenuated in β_6-null mice during bleomycin-induced lung fibrosis (19). Thus osteopontin appears to function downstream of the β_6-integrin in this response perhaps contributing to TGF-β1 activation. The mechanism by which osteopontin participates in the activation of TGF-β1 is unknown.

The gelatinases, MMP-2 and MMP-9, are expressed during lung fibrosis and can degrade gelatin and collagen as well as activate TGF-β and regulate cellular recruitment (6, 15, 23, 40). Our findings of reduced MMP-2 expression and activation in osteopontin −/− mice when challenged with bleomycin are supported by in vitro work that shows that osteopontin can induce and activate MMP-2 in carcinoma cell lines (34, 35). A recent study showed that transgenic mice overexpressing osteopontin develop arterial intimal thickening with increased expression and activation of MMP-2 (18). Similar to osteopontin, MMP-2 expression peaks during later stages of lung fibrosis and lung epithelia, including hyperplastic type II cells, which are a prominent source of MMP-2 in both UIP and murine models of fibrosis initiated by intratracheal bleomycin (15, 23). These data suggest that osteopontin and MMP-2 function at similar stages of lung fibrosis and that MMP-2 expression may be regulated by osteopontin during lung injury in vivo. Osteopontin can induce the expression of both membrane-type MMP-1 (MMP-14) and tissue inhibitor of metalloproteinases-2 and thus regulate MMP-2 activation in vitro (34). Interestingly, active MMP-2 is among the proteases with the capacity to activate TGF-β1 and it is therefore possible that impaired TGF-β1 activation could reflect deficient MMP-2 activity in osteopontin −/− mice (40). Further studies are necessary to clarify the role of osteopontin in regulating TGF-β1 and MMP-2 expression and activation in the lung. Nevertheless, the closely related expression pattern of osteopontin with TGF-β1 and MMP-2 supports a potentially important role for osteopontin in lung repair and fibrosis.

ACKNOWLEDGMENTS

We acknowledge E. Lucey for technical assistance in administering bleomycin to the mice and K. Singh for technical assistance with immunohistochemical staining for type I collagen.

GRANTS

This work was supported by Grants HL-04343 and HL-63339 from the National Institutes of Health.

REFERENCES

1. **American Thoracic Society/European Respiratory Society International Multidisciplinary Consensus.** Classification of the idiopathic interstitial pneumonias. *Am J Respir Crit Care Med* 165: 277–304, 2002.
2. **Annes JP, Munger JS, and Rifkin DB.** Making sense of latent TGF-β activation. *J Cell Sci* 116: 217–224, 2003.
3. **Antoniades HN, Bravo MA, Avila RE, Galanopoulos T, Neville-Golden J, Maxwell M, and Selman M.** Platelet-derived growth factor in idiopathic pulmonary fibrosis. *J Clin Invest* 86: 1055–1064, 1990.
4. **Ashcroft T, Simpson JM, and Timbrell V.** Simple method of estimating severity of pulmonary fibrosis on a numerical scale. *J Clin Pathol* 41: 467–470, 1988.
5. **Ashkar S, Weber GF, Panoutsakopoulou V, Sanchirico ME, Jansson M, Zawaideh S, Rittling SR, Denhardt DT, Glimcher MJ, and Cantor H.** Eta-1 (osteopontin): an early component of type I (cell-mediated) immunity. *Science* 287: 860–864, 2000.
6. **Betsuyaku T, Fukuda Y, Parks WC, Shipley JM, and Senior RM.** Gelatinase B is required for alveolar bronchiolization after intratracheal bleomycin. *Am J Pathol* 157: 525–535, 2000.
7. **Borzone G, Moreno R, Urrea R, Meneses M, Oyarzun M, and Lisboa C.** Bleomycin-induced chronic lung damage does not resemble human idiopathic pulmonary fibrosis. *Am J Respir Crit Care Med* 163: 1648–1653, 2001.
8. **Brown LF, Berse B, Van de Water L, Papadopoulos-Sergiou A, Perruzzi CA, Manseau EJ, Dvorak HF, and Senger DR.** Expression and distribution of osteopontin in human tissues: widespread association with luminal epithelial surfaces. *Mol Biol Cell* 3: 1169–1180, 1992.
9. **Chabas D, Baranzini SE, Mitchell D, Bernard CC, Rittling SR, Denhardt DT, Sobel RA, Lock C, Karpuj M, Pedotti R, Heller R, Oksenberg JR, and Steinman L.** The influence of the proinflammatory cytokine, osteopontin, on autoimmune demyelinating disease. *Science* 294: 1731–1735, 2001.
10. **Chomczynski P and Sacchi N.** Single-step method of RNA isolation by acid guanidinium thiocyanate-phenol-chloroform extraction. *Anal Biochem* 162: 156–159, 1987.
11. **Denhardt DT, Noda M, O'Regan AW, Pavlin D, and Berman JS.** Osteopontin as a means to cope with environmental insults: regulation of inflammation, tissue remodeling, and cell survival. *J Clin Invest* 107: 1055–1061, 2001.
12. **Fagenholz PJ, Warren SM, Greenwald JA, Bouletreau PJ, Spector JA, Crisera FE, and Longaker MT.** Osteoblast gene expression is differentially regulated by TGF-β isoforms. *J Craniomaxillofac Surg* 12: 183–190, 2001.
13. **Genovese C, Rowe D, and Kream B.** Construction of DNA sequences complementary to rat α_1 and α_2 collagen mRNA and their use in studying the regulation of type I collagen synthesis by 1,25-dihydroxyvitamin D. *Biochemistry* 23: 6210–6216, 1984.
14. **Hallahan DE, Geng L, and Shyr Y.** Effects of intercellular adhesion molecule 1 (ICAM-1) null mutation on radiation-induced pulmonary fibrosis and respiratory insufficiency in mice. *J Natl Cancer Inst* 94: 733–741, 2002.
15. **Hayashi T, Stetler-Stevenson WG, Fleming MV, Fishback N, Koss MN, Liotta LA, Ferrans VJ, and Travis WD.** Immunohistochemical study of metalloproteinases and their tissue inhibitors in the lungs of patients with diffuse alveolar damage and idiopathic pulmonary fibrosis. *Am J Pathol* 149: 1241–1256, 1996.
16. **Huang M, Sharma S, Zhu LX, Keane MP, Luo J, Zhang L, Burdick MD, Lin YQ, Dohadwala M, Gardner B, Batra RK, Strieter RM, and Dubinett SM.** IL-7 inhibits fibroblast TGF-β production and signaling in pulmonary fibrosis. *J Clin Invest* 109: 931–937, 2002.
17. **Hullinger TG, Pan Q, Viswanathan HL, and Somerman MJ.** TGF-β and BMP-2 activation of the osteopontin promoter: roles of smad- and hox-binding elements. *Exp Cell Res* 262: 69–74, 2001.
18. **Isoda K, Nishikawa K, Kamezawa Y, Yoshida M, Kusuhara M, Moroi M, Tada N, and Ohsuzu F.** Osteopontin plays an important role in the development of medial thickening and neointimal formation. *Circ Res* 91: 77–82, 2002.
19. **Kaminski N, Allard JD, Pittet JF, Zuo F, Griffiths MJ, Morris D, Huang X, Sheppard D, and Heller RA.** Global analysis of gene expression in pulmonary fibrosis reveals distinct programs regulating lung inflammation and fibrosis. *Proc Natl Acad Sci USA* 97: 1778–1783, 2000.
20. **Khalil N, O'Connor RN, Flanders KC, and Unruh H.** TGF-β_1, but not TGF-β_2 or TGF-β_3, is differentially present in epithelial cells of advanced

pulmonary fibrosis: an immunohistochemical study. *Am J Respir Cell Mol Biol* 14: 131–138, 1996.
21. **Krishna G, Liu K, Shigemitsu H, Gao M, Raffin TA, and Rosen GD.** PG490–88, a derivative of triptolide, blocks bleomycin-induced lung fibrosis. *Am J Pathol* 158: 997–1004, 2001.
22. **Kunkel SL, Lukacs NW, Strieter RM, and Chensue SW.** Th1 and Th2 responses regulate experimental lung granuloma development. *Sarcoidosis Vasc Diffuse Lung Dis* 13: 120–128, 1996.
23. **Kunugi S, Fukuda Y, Ishizaki M, and Yamanaka N.** Role of MMP-2 in alveolar epithelial cell repair after bleomycin administration in rabbits. *Lab Invest* 81: 1309–1318, 2001.
24. **Liaw L, Birk D, Ballas C, Whitsitt J, Davidson J, and Hogan B.** Altered wound healing in mice lacking a functional osteopontin gene (spp1). *J Clin Invest* 101: 1468–1478, 1998.
26. **Michon IN, Penning LC, Molenaar TJ, van Berkel TJ, Biessen EA, and Kuiper J.** The effect of TGF-β receptor binding peptides on smooth muscle cells. *Biochem Biophys Res Commun* 293: 1279–1286, 2002.
27. **Morris DG, Huang X, Kaminski N, Wang Y, Shapiro SD, Dolganov G, Glick A, and Sheppard D.** Loss of integrin α(v)β6-mediated TGF-β activation causes Mmp12-dependent emphysema. *Nature* 422: 169–173, 2003.
28. **Nakama K, Miyazaki Y, and Nasu M.** Immunophenotyping of lymphocytes in the lung interstitium and expression of osteopontin and interleukin-2 mRNAs in two different murine models of pulmonary fibrosis. *Exp Lung Res* 24: 57–70, 1998.
29. **Niewoehner DE and Hoidal JR.** Lung fibrosis and emphysema: divergent responses to a common injury? *Science* 217: 359–360, 1982.
30. **Ophascharoensuk V, Giachelli CM, Gordon K, Hughes J, Pichler R, Brown P, Liaw L, Schmidt R, Shankland SJ, Alpers CE, Couser WG, and Johnson RJ.** Obstructive uropathy in the mouse: role of osteopontin in interstitial fibrosis and apoptosis. *Kidney Int* 56: 571–580, 1999.
31. **O'Regan AW, Chupp GL, Lowry JA, Goetschkes M, Mulligan N, and Berman JS.** Osteopontin is associated with T cells in sarcoid granulomas and has T cell adhesive and cytokine-like properties in vitro. *J Immunol* 162: 1024–1031, 1999.
32. **O'Regan AW, Hayden JM, Body S, Liaw L, Mulligan N, Goetschkes M, and Berman JS.** Abnormal pulmonary granuloma formation in osteopontin-deficient mice. *Am J Respir Crit Care Med* 164: 2243–2247, 2001.
33. **O'Regan AW, Nau GJ, Chupp GL, and Berman JS.** Osteopontin (Eta-1) in cell-mediated immunity: teaching an old dog new tricks. *Immunol Today* 21: 475–478, 2000.
34. **Philip S, Bulbule A, and Kundu GC.** Osteopontin stimulates tumor growth and activation of promatrix metalloproteinase-2 through nuclear factor-κB-mediated induction of membrane type I matrix metalloproteinase in murine melanoma cells. *J Biol Chem* 276: 44926–44935, 2001.
35. **Philip S and Kundu GC.** Osteopontin induces nuclear factor-kB-mediated promatrix metalloproteinase-2 activation through IkB α/IKK signaling pathways and curcumin (diferulolylmethane) downregulates these pathways. *J Biol Chem* 278: 14487–14497, 2003.
36. **Selman M, King TE, and Pardo A.** Idiopathic pulmonary fibrosis: prevailing and evolving hypotheses about its pathogenesis and implications for therapy. *Ann Intern Med* 134: 136–151, 2001.
37. **Takahashi F, Takahashi K, Okazaki T, Maeda K, Ienaga H, Maeda M, Kon S, Uede T, and Fukuchi Y.** Role of osteopontin in the pathogenesis of bleomycin-induced pulmonary fibrosis. *Am J Respir Cell Mol Biol* 24: 264–271, 2001.
38. **Trueblood NA, Xie Z, Communal C, Sam F, Ngoy S, Liaw L, Jenkins AW, Wang J, Sawyer DB, Bing OH, Apstein CS, Colucci WS, and Singh K.** Exaggerated left ventricular dilation and reduced collagen deposition after myocardial infarction in mice lacking osteopontin. *Circ Res* 88: 1080–1087, 2001.
39. **Weber GF, Zawaideh S, Hikita S, Kumar VA, Cantor H, and Ashkar S.** Phosphorylation-dependent interaction of osteopontin with its receptors regulates macrophage migration and activation. *J Leukoc Biol* 72: 752–761, 2002.
40. **Yu Q and Stamenkovic I.** Cell surface-localized matrix metalloproteinase-9 proteolytically activates TGF-β and promotes tumor invasion and angiogenesis. *Genes Dev* 14: 163–176, 2000.
41. **Zuo F, Kaminski N, Eugui E, Allard J, Yakhini Z, Ben-Dor A, Lollini L, Morris D, Kim Y, DeLustro B, Sheppard D, Pardo A, Selman M, and Heller RA.** Gene expression analysis reveals matrilysin as a key regulator of pulmonary fibrosis in mice and humans. *Proc Natl Acad Sci USA* 99: 6292–6297, 2002.